Soft Matter

Wettability-Tuned Silica Particles for Emulsion-Templated Microcapsules

Journal:	*Soft Matter*
Manuscript ID	SM-ART-06-2023-000860.R1
Article Type:	Paper
Date Submitted by the Author:	15-Sep-2023
Complete List of Authors:	Starvaggi, Nicholas; Texas A&M University System, Chemistry Bradford, Braden; Texas A&M University System, Materials Science and Engineering Taylor, Cameron; Texas A&M University System, Materials Science & Engineering Pentzer, Emily; Texas A&M University System, Chemistry, Materials Science & Engineering

Wettability-Tuned Silica Particles for Emulsion-Templated Microcapsules

Nicholas C. Starvaggi,[1] B. Jack Bradford,[2] Cameron D.L. Taylor,[2] Emily B. Pentzer*[1,2]

[1]Dept. of Chemistry, Texas A&M University, College Station, TX 77843
[2]Dept. of Materials Science & Engineering, Texas A&M University, College Station, TX 77843
*Correspondence: emilypentzer@tamu.edu

Abstract

Pickering emulsions play a significant role in generating advanced materials and have widespread application in personal care products, consumer goods, crude oil refining, energy management, etc. Herein we report a class of wettability tuned silica-based Pickering emulsifiers which stabilize a diverse range of fluid-fluid interfaces: oil/water, ionic liquid/oil, and oil/oil, and their use to prepare microcapsules via interfacial polymerization. To alter particle wettability, colloidal suspensions of SiO_2 particles (22 nm) were modified via silanization with reagents of varied hydrophilicity/hydrophobicity, giving particles that could be dispersed in solvents that became the continuous phase of the emulsions. To test the viability of this system as templates for the fabrication of composite materials, the different particle-stabilized emulsions were coupled with interfacial polymerization, leading to microcapsules with polyurea/silica shells. These results demonstrate that a single particle feedstock can be coupled with fundamental chemical transformation to access a versatile toolkit for the stabilization of diverse fluid interfaces and serve as a template for the preparation of hybrid architectures.

Introduction

Fluid-filled microcapsules find widespread application in biomedicine,[1] cosmetics,[2] foodstuffs,[3] and energy management,[4] among other industries. Commonly spherical and tens of microns in diameter, microcapsules comprise a liquid core surrounded by a shell material (e.g., polymer or carbon).[5] Encapsulation imparts thermal stability to the core, resistance to leakage, and enhanced protection against undesired reactions with external agents.[6] Additionally, encapsulation resolves challenges with bulk active liquid processing (e.g., high viscosity) and increases the active surface area, which may assist in the mass transfer of small molecules across the interface.[7] Most commonly, encapsulation may be accomplished via hard-template approach, wherein a polymer shell is grown around a sacrificial core (e.g., layer-by-layer assembly atop a silica particle),[8] or via soft-template approach, which utilizes a stable biphasic system (e.g., interfacial polymerization in emulsions).[9] Both cases enable the handling of fluids as solid powders, which facilitates their use in specialized applications like direct air capture of CO_2,[10,11] contaminant removal,[9,12] and targeted drug delivery.[13,14]

The emulsion-based approach for encapsulation has garnered increased attention over the past several decades.[15] Being mixtures of immiscible fluids, emulsions are thermodynamically unstable

and tend to macrophase separate over time, yielding, for example, an oil phase atop of water.[16] To stabilize emulsion droplets against coalescence, small molecule surfactants (e.g., sodium dodecyl sulfate)[17] or surface-active polymers (e.g., PEO-PPO-PEO block copolymers)[18] have been employed to minimize the interfacial tension between the phases. In complement to these systems, Ramsden and Pickering recognized the role of finely divided particles in stabilizing emulsions in the early twentieth century.[19,20] These so-called Pickering emulsions have since demonstrated unusually high stability against droplet coalescence and generally have lower toxicity compared to traditionally-stabilized emulsions.[21] Common Pickering surfactants include pristine or alkylated graphene oxide nanosheets,[22–24] exfoliated clay nanosheets,[25] cellulose nanocrystals,[26] and surface-modified silica particles.[27]

Of the varied particles that serve as surfactants, colloidal silica (SiO_2) particles are chemically stable and relatively simple to covalently functionalize via known techniques. For emulsion systems, particle wettability is characterized by the contact angle theta (θ) formed by the particle at the interface of the two immiscible fluids. Per the Bancroft rule, hydrophilic particles ($\theta < 90°$) prefer contact with the aqueous phase, inducing the formation of an oil-in-water (o/w) emulsion, whereas hydrophobic particles ($\theta > 90°$) favor contact with the nonpolar phase, generating water-in-oil (w/o) emulsions (**Figure 1**).[28,29] In pioneering work, Binks and colleagues systematically investigated various factors that impact SiO_2-stabilized Pickering emulsions, including pH, particle concentration, and salinity. Pristine SiO_2 particles, for example, are too hydrophilic to stabilize Pickering emulsions due to the negative surface charge and electrostatic repulsion between particles; consequently, appropriate surface modification of neat silica is needed for emulsion stabilization.[30] The central role of particle wettability in the preparation of Pickering emulsions has inspired numerous studies to investigate this phenomenon. Sadeghpour and colleagues modified SiO_2 particles in dispersion via adsorption of oleic acid to surface silanol groups (e.g., via hydrogen bonding); this increased hydrophobicity and led to the stabilization of oil-in-water emulsions.[31] Further, Saigal and coworkers modified SiO_2 particles with poly(2-(dimethylamino)ethyl methacrylate) brushes grafted from surface via atom-transfer radical polymerization (ATRP), increasing particle hydrophobicity and thereby conferring the ability to stabilize cyclohexane-in-water and xylene-in-water emulsions.[32] As such, most previous reports provide a particle modification strategy customized for a specific interface. However, the ability to tune particle wettability via a common chemical process to stabilize a range of emulsions (i.e., hydrocarbon-in-water, ionic liquid-in-oil, polar oil-in-oil) is, to the best of our knowledge, unreported. Such a toolkit would enable researchers to prepare a variety of different composite structures, including microcapsules by interfacial polymerization with the dispersed phase serving as the liquid core.

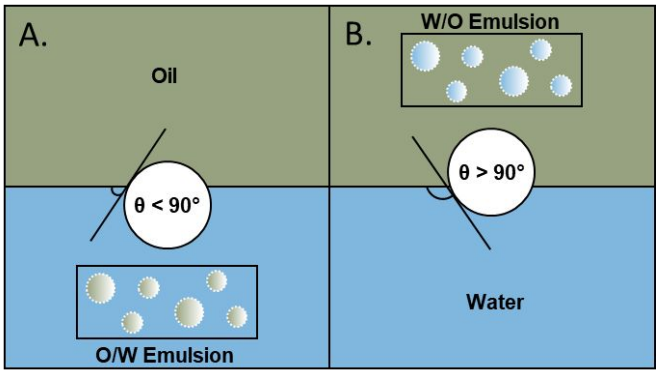

Figure 1. Illustration of contact angle (θ) made by (A) hydrophilic and (B) hydrophobic particles at an oil-water interface and the types of emulsions they stabilize.

Herein, we report a class of SiO_2-based Pickering emulsifiers, modified via fundamental chemical transformation to stabilize a diverse range of fluid-fluid interfaces, and the use of these emulsions to prepare microcapsules. Our focus is to provide a facile route to modify particles to stabilize a variety of fluid-fluid interfaces in Pickering emulsions and leverage these phase-separated systems for microcapsule formation, as relevant to critical applications such as direct air capture, thermal energy management, and contaminant removal. Colloidal SiO_2 particles were functionalized with silane reagents of varied hydrophilicity/hydrophobicity to prepare particles with different wettabilities, as confirmed by sessile drop experiments. These particles demonstrated distinct dispersibility, interfacial activity, and the ability to stabilize different emulsions, generating hydrocarbon-in-water, ionic liquid-in-toluene, and polar oil-in-octane emulsions. To further probe interfacial dynamics, pendant drop tensiometry was employed to investigate the hydrocarbon-water interface at equilibrium with and without particle surfactants dispersed in the continuous phase. We then coupled these particle-stabilized emulsions with interfacial polymerization to yield microcapsules with a polyurea/silica composite shell and core liquid of the dispersed phase. This study demonstrates that application of the same chemical process can generate a versatile toolkit to stabilize different fluid-fluid interfaces, which can then serve as a template for the construction of hybrid architectures.

Experimental Section

Materials. LUDOX® TMA colloidal silica (34 wt% suspension in H_2O, 7631-86-9), sodium dodecyl sulfate (151-21-3), (3-aminopropyl)trimethoxysilane (97%, 13822-56-5), trimethoxy(octyl)silane (96%, 3069-40-7), trimethoxy(octadecyl)silane (technical grade, 3069-42-9), ethylenediamine (EDA, ≥99%, 107-15-3), 1,6-hexanediisocyanate (HDI, ≥99%, 822-06-0), propylamine (107-10-8), potassium bromide (FTIR grade, ≥99%, 7758-02-3), acetone (67-64-1), and hexanes (110-54-3) were obtained from MilliporeSigma. Trimethoxy(methyl)silane (98.0+%, 1185-55-3), trimethoxy(propyl)silane (98%, 1067-25-0), *N*,*N*-dimethylformamide (68-12-2), and toluene (108-88-3) were obtained from Fischer Scientific. Ammonium hydroxide (28-30%

solution in water, ACS reagent, 1336-21-6) and n-octane (111-65-9) were obtained from Oakwood Chemical. Mesitylene (108-67-8) was obtained from Acros Organics, 1-butyl-3-methylimidazolium hexafluorophosphate ([BMIM][PF_6], 99%, 174501-64-5) was obtained from Iolitec, ethanol (200 proof, 64-17-5) was acquired from VWR, and acetone-d6 (666-52-4) was obtained from Cambridge Isotope. Poly(α-olefin)$_{432}$ (PAO_{432}) was received from ExxonMobil and Chevron Phillips Chemical Company. All chemicals were used as received without further purification.

Instrumentation. Emulsification was accomplished with a BioSpec Products Inc. hand-held emulsifier (model number 985370). Centrifugation was completed with a Thermo Scientific Sorvall ST 8 centrifuge. Ultrasonication was completed with a QSonica Q55 Sonicator, bath sonication was accomplished with a Fisherbrand CPX3800 Ultrasonic Bath 5.7 L, and vortex mixing was completed with a Fisherbrand vortex mixer. Fourier transform infrared spectroscopy (FTIR) was collected in ATR or transmission mode, depending on the sample. For ATR mode, a JASCO FT/IR-4600 with a ZnSe/diamond prism was used with 32 scans per sample. For transmission mode, a Thermo Nicolet 6700 FTIR equipped with a liquid-nitrogen-cooled MCT A (HgCdTe) detector was used with 64 scans at a resolution of 1 cm^{-1}. Approximately 5 mg of sample was added to 100 mg of KBr in a mortar, ground into a uniform powder with a pestle, then pressed into a pellet using a Specac 15 Ton Hydraulic KBr Press. ^{1}H NMR nuclear magnetic resonance spectroscopy was carried out using a Bruker Avance NEO 400 mHz NMR spectrometer and residual solvent used as reference. Thermogravimetric analysis was carried out using TA Instruments TGA 5500 (under N_2, ramp 20 °C/min to 900 °C). Contact angle determination was accomplished using sessile drop technique with a contact angle/pendant drop goniometer (DataPhysics OCA 11). To produce a flat surface, samples were pressed into a 7 mm KBr pellet die set. A 1 μL droplet of deionized water was gently deposited on the sample and the air-droplet-substrate contact angle was measured by the software. All reported measurements represent an average of five trials. Pendant drop tensiometry was completed on the same instrument. A droplet of PAO_{432}, held by a U-shaped blunt-tipped needle, was dispersed in a continuous phase of pure, deionized water (for measuring interfacial effects without particle surfactants) or containing 1 mg/mL suspended SiO_2-NH_2. The oil droplet was filled to 45 μL at a rate of approximately 0.5 μL/s. Optical microscopy images were taken using an AmScope 150C-2L microscope equipped with an 18 MP USB 3.0 camera. To prepare emulsions for imaging, one drop of emulsion sample was placed on a glass slide and diluted with one drop of continuous phase. Particle size analysis was completed on a Horiba Partica LA-960 particle sizer. For modified silica particles, a small sample (<50 mg) was dispersed in an appropriate solvent and ultrasonicated at 30% amplitude for at least 15 min prior to characterization. For microcapsules, a small sample (<50 mg) was gently dispersed in methanol. Analysis was accomplished via laser diffraction, while the sample was under magnetic stirring. Scanning electron microscopy (SEM) images were taken using a TESCAN VEGA SEM with an accelerating voltage of 10 kV. SEM samples were sputter coated with 10 nm of Au prior to imaging.

Particle Functionalization. LUDOX® TMA colloidal silica was functionalized per a modified method reported by Schoth and colleagues.[33] Silica suspension (50 mL), ethanol (50 mL), and sodium dodecyl sulfate (50 mg) were charged to a 250 mL round-bottom flask with a large stir bar. Under vigorous stirring, the pH of the mixture was raised from approximately 7.5 to 9.0 via dropwise addition of aqueous ammonium hydroxide. Excess silane reagent (0.02 mol) [(3-aminopropyl)trimethoxysilane, trimethoxy(methyl)silane, trimethoxy(propyl)silane, trimethoxy(octyl)silane, or trimethoxy(octadecyl)silane] was added dropwise and the dispersion was stirred for 24 h under ambient conditions to allow equilibration. After 24 h, additional ethanol (~100 mL) was added to overcome any gelation that occurred overnight. The temperature was then increased to 80 °C and the mixture was refluxed for 2 h. Modified particles were isolated via centrifugation (4500 rpm, 30 min), washed thrice with acetone, and dried in vacuo overnight. Of note, for the SiO_2-C1 synthesis, modified silica remained dispersed after extended centrifugation; thus, particles were first isolated by solvent evaporation under reduced pressure and then washed/dried as described above.

Emulsion Preparation. Suspensions of modified SiO_2 particles were prepared by adding an appropriate amount of SiO_2-NH_2 or SiO_2-C1 to distilled water, SiO_2-C3 to toluene, and SiO_2-C8 or SiO_2-C18 to octane. All suspensions were ultrasonicated at 30% amplitude for at least 30 min prior to use to ensure particle dispersion. To generate an emulsion, unless otherwise stated, 5 mL of continuous phase containing 5 wt% functionalized silica was added to a vial, followed by 1 mL of dispersed phase (PAO_{432}, [BMIM][PF_6], or DMF). The resulting mixture was emulsified with a hand-held emulsifier for three cycles of 20 s on followed by 5 s off.

Microcapsule Synthesis. Emulsions were prepared as detailed above, with the exception that HDI or EDA was added to the PAO_{432}, [BMIM][PF_6], or DMF (see **Table S1** for detailed amounts). After emulsification, an additional 1 mL of continuous phase was added to dilute the emulsion, then a solution of the complementary monomer to what was in the discontinuous phase (i.e., HDI or EDA) diluted with 1.25 mL of continuous phase was added dropwise with gentle hand swirling. The emulsion was allowed to stand undisturbed for 72 h. Then, the reaction mixture was added to 100 mL of distilled water or hexane (depending on the continuous phase identity) and quenched via addition of 7 mL propylamine to ensure complete reaction with any residual isocyanate groups. After 5 h, quenched microcapsules were then isolated via gravity filtration and washed again with distilled water or hexanes until the supernatant was neutral, as determined by litmus test. Finally, microcapsules were dried in vacuo overnight, resulting in a white powder.

Determination of [BMIM][PF_6] Weight Percent of Microcapsules via ^{1}H NMR. Per a previously reported procedure,[11] approximately 20 mg of the [BMIM][PF_6] microcapsules were added to a vial containing a 0.039 M solution of mesitylene (internal standard) in acetone-d6. The mixture was then sonicated/vortex mixed to extract all [BMIM][PF_6] from the microcapsule core. Next,

the solution was passed through a poly(tetrafluoroethylene) syringe filter (0.45 μm pore size) to remove the broken shell material and the eluent placed in an NMR tube for ^{1}H NMR analysis. Weight percent encapsulated [BMIM][PF_6] was then determined by comparing the relative integration of the methyl peak from mesitylene (2.09 ppm) to the methyl peak of the [BMIM] cation (3.93 ppm) (**Figure S1**). This procedure was replicated thrice.

Determination of PAO_{432} Weight Percent of Microcapsules via Mass Difference. Hexanes (10 mL) was added to 70 mg PAO_{432} microcapsules. This mixture was sonicated/vortex mixed to extract the PAO_{432} from the microcapsule core. The solution was then passed through a poly(tetrafluoroethylene) syringe filter (0.45 μm pore size) into a tared vial to remove the broken shell material. Hexanes was removed from the mixture via rotary evaporation, leaving behind PAO_{432} as a viscous oil. The mass of this oil was determined and then compared to the initial microcapsule mass to determine weight percent. This procedure was replicated thrice.

Results & Discussion

To achieve a family of particle surfactants with a range of wettability, SiO_2 particles (22 nm in diameter) in aqueous suspension were functionalized through a modified procedure, based on that reported by Schoth and colleagues.[33] This method was selected over other modification routes (e.g., drying and resuspending in an organic solvent), as a recent study found that functionalization at lower pH (~8.5) led to weaker silica-silane bonding at the LUDOX surface and resulting in interfacially inactive particles.[34] Thus, an aqueous solution of LUDOX TMA SiO_2 was diluted in ethanol and reacted with excess silane for 24 h. It is commonly accepted that surface functionalization occurs by a combination of base-catalyzed hydrolysis of a trimethoxy silane and subsequent condensation with surface silanol groups on the colloidal SiO_2 particles, leading to covalent attachment of the silane to the particle surface (**Figure 2A**).[35] Particles modified with amino, methyl, propyl, octyl, or octadecyl trimethoxysilane are named SiO_2-NH_2, SiO_2-C1, SiO_2-C3, SiO_2-C8, or SiO_2-C18, respectively.

Modified particles were characterized via laser diffraction, Fourier-transform infrared (FTIR) spectroscopy, and thermogravimetric analysis (TGA). Individual colloid size (22 nm) is not expected to change significantly during silanization; however, modified particles exhibit an average size of 0.2-12.2 μm (**Figure S2)**. We attribute this apparent size increase to particle aggregation during drying. Particle modification was confirmed via FTIR spectroscopy (**Figure 2B**). All samples of modified particles show three characteristic FTIR stretching frequencies: Si-O-Si (~1100 cm^{-1}), Si-OH (~955 cm^{-1}), and broad O-H (~3500 cm^{-1}). Notably, the presence of the O-H stretching frequency indicates the presence of residual silanol and/or adsorbed water. The spectrum of the SiO_2-NH_2 particles reveals the appearance of a stretching frequency due to sp^3 C-H group at ~2900 cm^{-1}; a peak at ~3300-3500 cm^{-1} would be expected due to the -NH_2 group but cannot be distinguished from O-H peak. In comparison to SiO_2-NH_2, intensity of the C-H peak increases significantly for SiO_2-C1, SiO_2-C3, SiO_2-C8, and SiO_2-C18 particles. Thermogravimetric analysis (TGA) was used to qualitatively characterize particle modification

(**Figure 2C**). Pristine SiO_2 particles are extremely hydroscopic due to the abundant silanol groups on the surface. Accordingly, most mass loss occurs < 100 °C and can be attributed to desorption of water. With the exception of SiO_2-C1, all functionalized samples demonstrate significantly lower mass loss below 100 °C, suggesting less adsorbed water than the pristine particles. The primary mass loss event for SiO_2-NH_2, SiO_2-C3, SiO_2-C8, and SiO_2-C18 occurs above 200 °C, which can be attributed to thermal degradation of grafted organic species.[36] SiO_2-C1 shows the lowest mass loss; though surprising, this is likely due to the loss mass of the organic component being obscured by the loss of water (though the particles have less water adsorbed than the pristine particles).

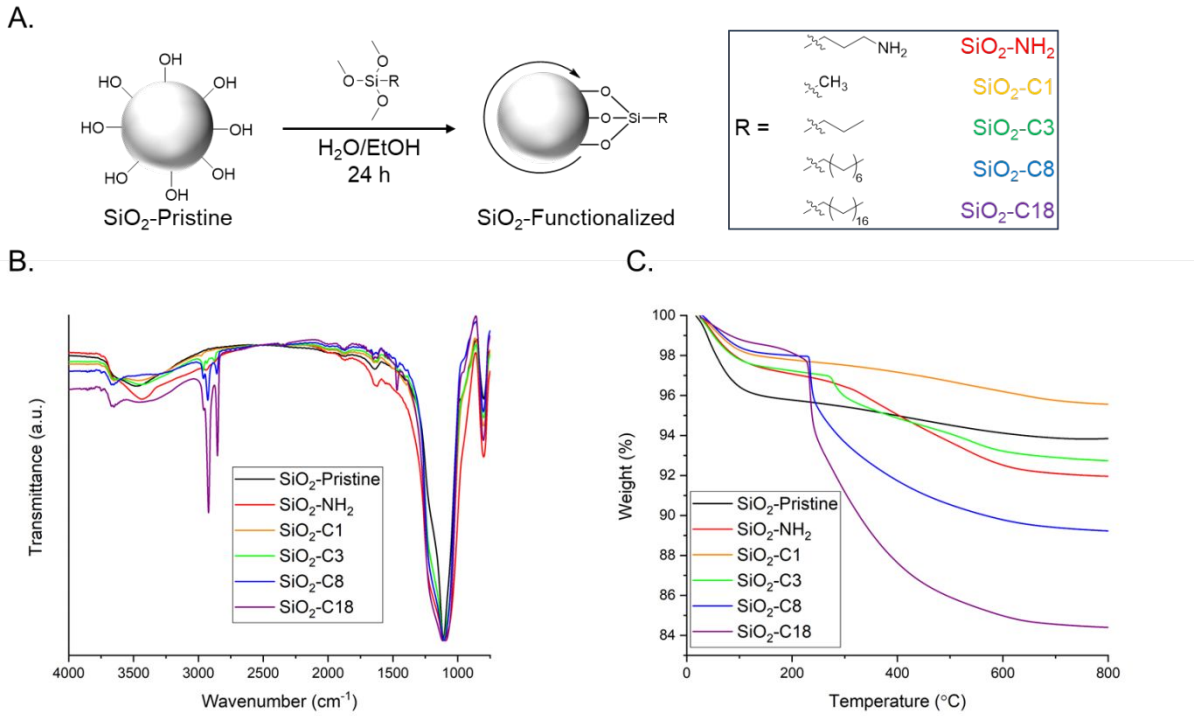

Figure 2. (A) Schematic demonstrating particle functionalization; (B) FTIR spectra and (C) TGA weight loss profiles of modified particle surfactants.

The sessile drop technique (e.g., static water contact angle) was used to characterize the relative wettability of silica particles and the five modified derivatives. As shown in **Figure 3A**, samples were prepared via compression of the particles into an FTIR window to generate a flat film of particles for characterization; of note, other methods such as plate compression led to surface defects and irreproducible results. Using a contact angle/pendant drop goniometer, a 1 µL droplet of water was deposited onto the sample and the contact angle measured. Pristine silica is so hydrophilic that the water droplet immediately spread across the surface and no measurement could be recorded. Similarly, for SiO_2-NH_2 and SiO_2-C1, the water droplet wet the entire surface and no contact angle could be measured, which we attribute to the hydrophilicity of the particles (**Figure S3**). However, particles functionalized of with longer alkyl chains led to measurable

contact angles, with the length of the alkyl chain dictating the hydrophobicity: SiO_2-C3 showed a contact angle of 98.0° ± 7.4° (**Figure 3B**), while SiO_2-C8 and SiO_2-C18 gave higher contact angles of 128.6° ± 1.6° and 129.1° ± 3.1°, respectively (**Figure 3C,D**). These measured contact angles were consistent across at least five samples of each particle type and highlight that particles coupled with longer alkyl chains are more hydrophobic, as expected.

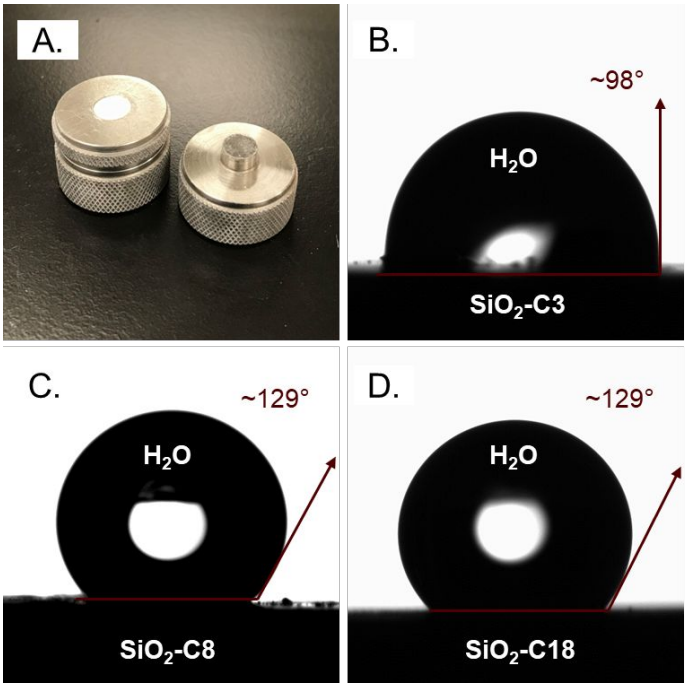

Figure 3. (A) Sessile drop preparation set-up; Contact angle determination for (B) SiO_2-C3, (C) SiO_2-C8, and (D) SiO_2-C18 particles.

Modified SiO_2 particles were investigated for capacity to stabilize different emulsion systems, with the approach that the solvent the particles are dispersible in would become the continuous phase. Pristine SiO_2 is dispersible in water but is too hydrophilic to adsorb to the fluid-fluid interface. In contrast, SiO_2-NH_2 and SiO_2-C1 are both dispersible in water and interfacially active. Addition of a hydrocarbon oil phase (e.g., PAO_{432}) to an aqueous dispersion of SiO_2-NH_2 or SiO_2-C1 followed by shear mixing led to a stable PAO_{432}-in-water emulsion (**Figure 4A, S4**), with the modified particles expected to reside at the fluid-fluid interface. Alternatively, the more hydrophobic SiO_2-C3 is dispersible in toluene and could be used to prepare emulsions with droplets of a hydrophilic fluid (e.g., [BMIM][PF_6]) in toluene (**Figure 4B**). Finally, SiO_2-C8 and SiO_2-C18 were both readily dispersible in the nonpolar oil octane, stemming from the longer alkyl chains grafted to the particle surface. Upon shear-mixing with a polar oil (e.g., DMF), oil-in-oil emulsions were realized (**Figure 4C, S4**). Of note, SiO_2-NH_2/SiO_2-C1 was too hydrophilic to stabilize the [BMIM][PF_6]-toluene or DMF-octane emulsion systems; modified particles migrated into the more polar phase upon shear-mixing, resulting in no emulsion formation for these combinations. Similarly, SiO_2-C8/SiO_2-C18 was too hydrophobic to stabilize PAO_{432}-in-H_2O or [BMIM][PF_6]-in-toluene

emulsions, demonstrating too high an affinity for PAO_{432} and toluene, respectively. All emulsions remained stable upon standing for at least two weeks, as confirmed by optical microscopy.

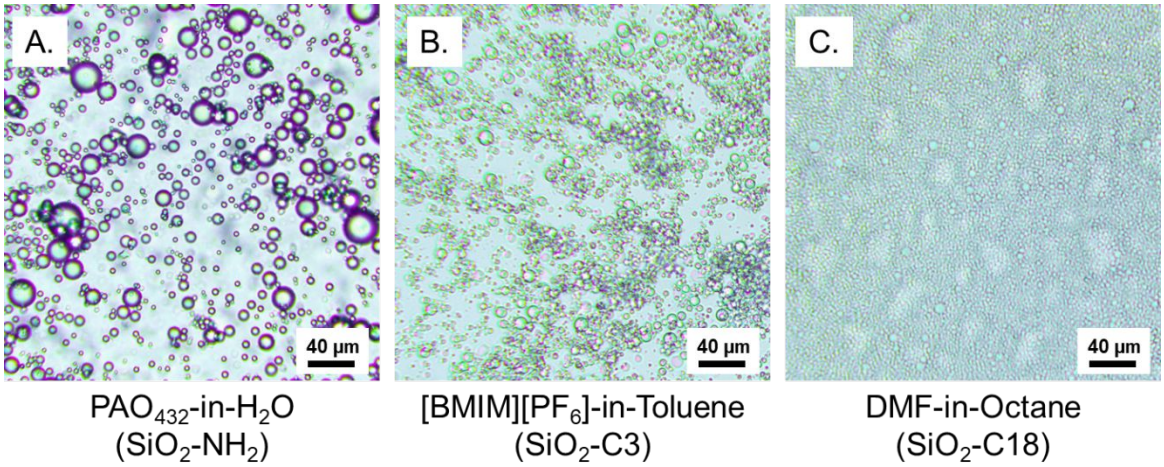

Figure 4. Optical microscopy images of emulsions stabilized by modified silica particles. (A) PAO_{432}-in-water stabilized by SiO_2-NH_2; (B) [BMIM][PF_6]-in-toluene stabilized by SiO_2-C3; (C) *N*,*N*-dimethylformamide-in-octane stabilized by SiO_2-C18.

From the images in **Figure 4**, qualitatively, a dramatic difference in droplet size across all three systems is observed. As the concentration of particles, energy input, and fluid-fluid ratios were consistent across all samples, we attribute this difference in droplet size to variations in the interfacial tension between the two fluids in each system. **Equation 1** relates droplet diameter to the emulsification energy input ($\tilde{\prod}$), interfacial tension (σ), and density of the continuous phase (ρ).[37] When power input is held constant, droplet diameter is expected to (i) increase with higher interfacial tension and/or decreased density and (ii) decrease under the opposite conditions. Interfacial tension in oil/water systems typically ranges from 30 – 50 mN/m, but is dramatically reduced for most oil-in-oil systems to 0 – 5 mN/m.[38] Our emulsion systems agree with this trend: the PAO_{432}-in-water system, having higher interfacial tension, gives larger droplets while the [BMIM][PF_6]- and DMF-in-oil systems exhibit significantly smaller droplets.

Equation 1. $d_{max} = \tilde{\prod}^{-2/5} \cdot \sigma^{3/5} \cdot \rho_c^{-1/5}$

To gain a better understanding of these systems, loading of the surfactant particles was varied from 0.5 to 5 wt% of the continuous phase volume, keeping the fluid-fluid ratio constant (**Figure S5**). For the PAO_{432}-in-H_2O and [BMIM][PF_6]-in-toluene emulsions, optical microscopy images support that droplet size decreased slightly as surfactant content is increased, reaching a plateau around 3 wt%. As the particle concentration is increased, more surfactant is available to reside at the fluid-fluid interface, resulting in smaller stable droplets. By contrast, larger and fewer droplets form when surfactant concentration is lowered. Interestingly, the DMF-in-octane emulsion does not appear to follow this general trend, showing droplets of varied sizes in all six images. We also

evaluated the impact of the phase volume with constant particle loading for the PAO_{432}-in-H_2O emulsion system (**Figure S6**). Binks and Lumsdon previously reported that oil-in-water emulsions catastrophically invert to water-in-oil at volume fractions of oil around 0.7,[39] and our experiments also find this trend: droplet size increases significantly from the 6:4 to 7:3 o/w emulsion systems, indicative of the phase inversion.

The role of interfacially active SiO_2 in lowering the interfacial tension (IFT) was investigated via pendant drop tensiometry. For these studies, the PAO_{432}-H_2O interface was selected as a model emulsion system and evaluated in the presence and absence of SiO_2-NH_2 particles in the aqueous phase. In the absence of a particle surfactant, the equilibrium IFT of the PAO_{432}-H_2O system was 39.76 ± 0.13 mN/m. This measurement represents the mean of the final twenty IFT data points from three consecutive trials, with propagated errors. When the water contained 1 mg/mL of SiO_2-NH_2 particles, the equilibrium IFT was reduced to 33.24 ± 0.17 mN/m (**Figure 5A**). This particle concentration was selected to maintain transparency of the continuous phase, allowing the goniometer to capture a clear image of the droplet profile and attain a precise IFT measurement. Of note, the *initial* IFT of the PAO_{432}-H_2O system, when measurement begins, is significantly lower than the particle-free system, suggesting rapid adsorption of the particles at the interface upon droplet formation. The first derivative of IFT with respect to droplet age for both systems is depicted in **Figure 5B.** Notably, the fastest rate of change of IFT for both systems occurs when the oil droplet is initially deposited in the continuous phase. In the first 4000 s, for example, the interface with SiO_2-NH_2 exhibits a broader 95% confidence interval (shaded) than the surfactant-free interface; these data indicate that the presence of SiO_2-NH_2 leads to highly variable rate of change which may be attributed to periodic and rapid particle rearrangement at the PAO_{432}-H_2O interface. **Figure 5C** shows an equilibrium droplet of PAO_{432} suspended in a water containing SiO_2-NH_2 (1 mg/mL). Remarkably, SiO_2-NH_2 particle aggregates can be observed at the PAO_{432}-H_2O interface: the apparently higher concentration of particles at the base of the droplet compared to the top half may be attributed to gravity. Taken with the observed particle aggregation in solution observed by light scattering studies, modified silica particles may assemble at the fluid-fluid interface in multilayers, providing a layered barrier to macrophase coalescence. Our ongoing work in this area is directed toward probing this hypothesis.

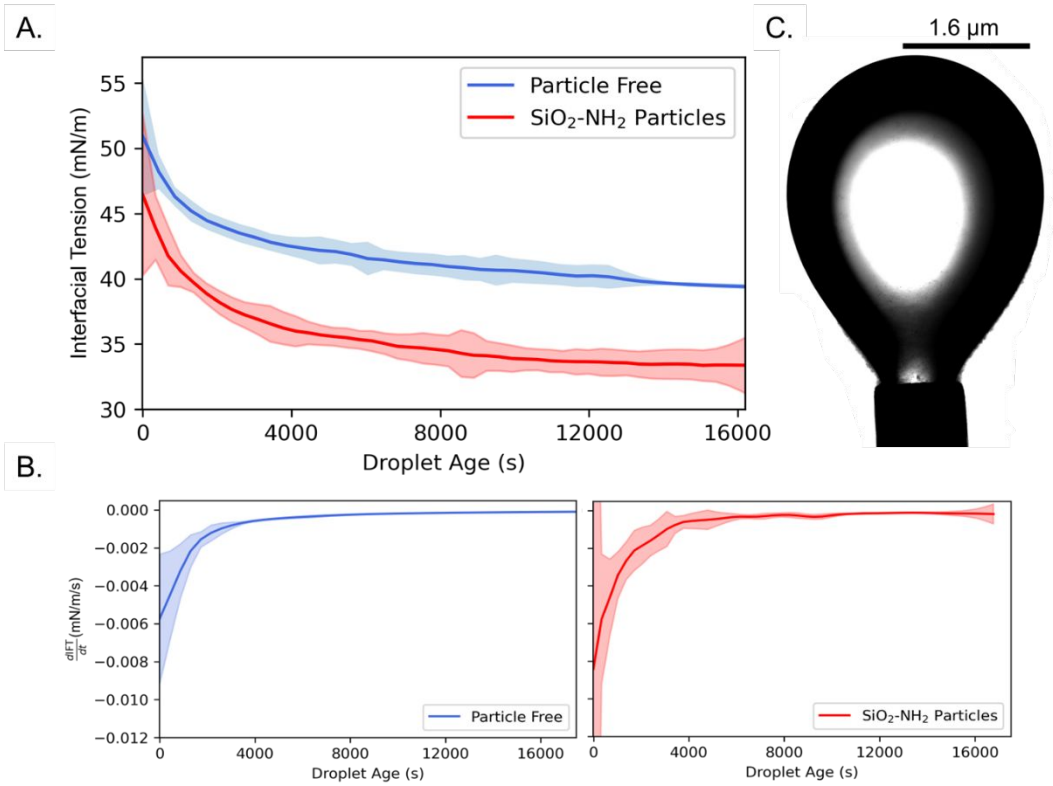

Figure 5. Pendant drop tensiometry measurements of PAO_{432} in deionized water. (A) IFT vs. time with and without SiO_2-NH_2; (B) The first derivative of IFT with respect to time; (C) Equilibrated PAO_{432} droplet with SiO_2-NH_2 at the hydrocarbon-water interface. Shaded regions represent the 95% confidence interval.

All emulsion systems were coupled with interfacial polymerization to produce microcapsules with a composite polyurea/silica shell and liquid core of the discontinuous phase (PAO_{432}, [BMIM][PF_6], or DMF). Interfacial polymerization is possible if one monomer (e.g., EDA) is in the polar phase and the second monomer (e.g., HDI) is in the nonpolar phase, resulting in step-growth polymerization at the interface, around the particle surfactants. Critically, excess monomer (either EDA or HDI, depending on the phase polarity) must be added to the continuous phase to avoid unreacted monomer in the core (**Table S1**). After 72 h, propylamine is added to quench any isocyanate groups and avoid inter-microcapsule fusing; microcapsules are then isolated by gravity filtration, gently washed to neutral pH with an appropriate solvent, and dried under vacuum.

Microcapsules were characterized by SEM, FTIR spectroscopy, and optical microscopy. As shown in **Figure 6A**, microcapsules prepared from the SiO_2-C3 stabilized [BMIM][PF_6]-in-toluene emulsion template exhibit rough surface morphology and nonuniform size distribution, common for microcapsules prepared from soft-template methods. **Table S2** summarizes microcapsule diameter, revealing a rough correlation between apparent emulsion droplet and microcapsule size (**Figure S7**). Typically, the larger droplets of the oil-in-water emulsion produced slightly larger microcapsules than those produced from the oil-in-oil emulsion, which may be indicative of

localization of polymerization. The FTIR spectra of the three types of microcapsules are shown in **Figure 6B**; stretching frequencies at 3400 cm^{-1} and 1600 cm^{-1} indicate the presence of N-H and C=O bonds of polyurea, respectively, and no stretching frequencies attributed to isocyanates are observed. Core identity can also be elucidated from these data. The strong sp^3 C-H stretching frequency at ~2900 cm^{-1} for the PAO_{432} microcapsules is indicative of the hydrocarbon core,[40] for example, while the [BMIM][PF_6] microcapsules demonstrate characteristic ionic liquid stretching frequencies at ~3200 cm^{-1}, ~1170 cm^{-1}, and ~800 cm^{-1}.[41] **Figure 6C** shows an optical microscopy image of PAO_{432}-filled microcapsules prepared from the SiO_2-NH_2 stabilized emulsions, and **Figure 6D** shows the same microcapsules after gentle compression. Also demonstrated in **Video 1**, upon compression, the core liquid (PAO_{432}) is expelled from the microcapsules, resulting in a dark wave that moves from right to left across the image. Extraction and characterization by mass difference or ^1H NMR was used to determine the loading of PAO_{432} and [BMIM][PF_6] in the respective capsules; in both cases, the capsules were 70-80 wt% of core liquid. Notably, for microcapsules with volatile cores (i.e., DMF), attempts to determine composition were not reliable, likely due to evaporation (**Table S3**).

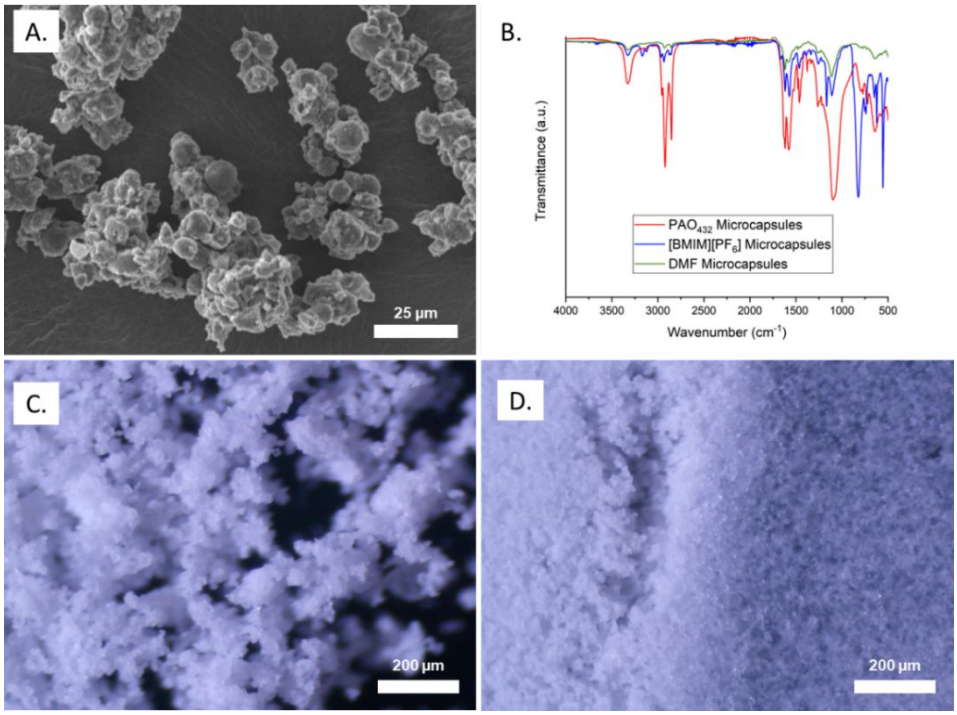

Figure 6. (A) SEM image of [BMIM][PF_6] microcapsules; (B) FTIR spectra of three different types of microcapsules; Optical microscopy images of PAO_{432} microcapsules (C) pre-compression and (D) post-compression.

Conclusions

In summary, silica particles were modified via silanization to obtain Pickering emulsifiers capable of stabilizing oil-in-water, ionic liquid-in-oil, and oil-in-oil emulsions. Silane reagents of varied hydrophobicity were chosen to impart particles with desired wettability, as confirmed by sessile

drop technique, and further supported by dispersibility in different solvents. Hydrophilic SiO_2-NH_2 and SiO_2-C1 particles had excellent dispersibility in water and could stabilize PAO_{432}-in-water emulsions, whereas the more hydrophobic SiO_2-C3 and SiO_2-C8/SiO_2-C18 particles were only dispersible in nonpolar solvents and were suitable for stabilizing ionic liquid-in-oil and oil-in-oil emulsions, respectively. The effect of SiO_2-NH_2 on the hydrocarbon-water interface was investigated via pendant drop tensiometry, revealing a dramatic reduction in IFT in the presence of the modified particles. These particle-stabilized systems were coupled with interfacial polymerization to yield microcapsules with a liquid core of the dispersed phase and a polyurea/silica shell; average microcapsule diameter showed reasonable correlation to emulsion droplet size. This demonstrates that the wettability and interfacial activity of silica particles can be readily tuned using a common modification approach, giving access to stable Pickering emulsions of different fluids and hybrid architectures for advanced applications. Our ongoing work in this area focuses on probing the interfacial dynamics of these systems and developing alternative particle surfactants (larger SiO_2 particles, anisotropic particles, etc.) to further elucidate the fundamental principles behind emulsion stabilization and destabilization. Additionally, we are applying these constructs for advanced applications, including separations, compartmentalized reactors, carbon capture, and lubricants.

Author Contributions

EP and NS conceived the research. NS performed all experiments and prepared the original manuscript draft. JB prepared select emulsions, collected optical microscopy images, and performed pendant drop tensiometry studies. CT took SEM images. All authors reviewed and edited. EP acquired funding for the research.

Conflicts of Interest

There are no conflicts to declare.

Acknowledgements

Use of the TAMU Materials Characterization Core Facility (RRID:SCR_022202), TAMU Soft Matter Facility (RRID:SCR_022482), and TAMU Microscopy & Imaging Center (RRID:SCR_022128) is acknowledged. The authors thank Dr. Peiran Wei for providing TGA and contact angle/pendant drop goniometer training, Dr. Wilson Serem for providing particle size analysis training, and Dr. Stanislav Vitha for assistance in taking SEM images. Additionally, the authors thank Dr. James Batteas for gracious use of his lab's FTIR spectrometer. NS is supported by an NSF Graduate Research Fellowship (Award #2139772) and CT is supported by a Gates Millennium Scholarship. EP thanks NSF DMR grant #2103182.

References

(1) Singh, M. N.; Hemant, K. S. Y.; Ram, M.; Shivakumar, H. G. Microencapsulation: A Promising Technique for Controlled Drug Delivery. *Res Pharm Sci* **2010**, *5* (2), 65–77.

(2) Casanova, F.; Santos, L. Encapsulation of Cosmetic Active Ingredients for Topical Application – a Review. *Journal of Microencapsulation* **2016**, *33* (1), 1–17. https://doi.org/10.3109/02652048.2015.1115900.
(3) F. Gibbs, Selim Kermasha, Inteaz Al, B. Encapsulation in the Food Industry: A Review. *International Journal of Food Sciences and Nutrition* **1999**, *50* (3), 213–224. https://doi.org/10.1080/096374899101256.
(4) Shchukina, E. M.; Graham, M.; Zheng, Z.; Shchukin, D. G. Nanoencapsulation of Phase Change Materials for Advanced Thermal Energy Storage Systems. *Chem. Soc. Rev.* **2018**, *47* (11), 4156–4175. https://doi.org/10.1039/C8CS00099A.
(5) Bentz, K. C.; Savin, D. A. Hollow Polymer Nanocapsules: Synthesis, Properties, and Applications. *Polym. Chem.* **2018**, *9* (16), 2059–2081. https://doi.org/10.1039/C8PY00142A.
(6) Wang, Y.; Starvaggi, N.; Pentzer, E. Capsules with Responsive Polymeric Shells for Applications beyond Drug Delivery. *Polym. Chem.* **2023**, *14* (35), 4033–4047. https://doi.org/10.1039/D3PY00434A.
(7) Luo, Q.; Pentzer, E. Encapsulation of Ionic Liquids for Tailored Applications. *ACS Appl. Mater. Interfaces* **2020**, *12* (5), 5169–5176. https://doi.org/10.1021/acsami.9b16546.
(8) Hong, J.; Han, J. Y.; Yoon, H.; Joo, P.; Lee, T.; Seo, E.; Char, K.; Kim, B.-S. Carbon-Based Layer-by-Layer Nanostructures: From Films to Hollow Capsules. *Nanoscale* **2011**, *3* (11), 4515. https://doi.org/10.1039/c1nr10575b.
(9) Luo, Q.; Wang, Y.; Chen, Z.; Wei, P.; Yoo, E.; Pentzer, E. Pickering Emulsion-Templated Encapsulation of Ionic Liquids for Contaminant Removal. *ACS Appl. Mater. Interfaces* **2019**, *11* (9), 9612–9620. https://doi.org/10.1021/acsami.8b21881.
(10) Lee, Y.-Y.; Edgehouse, K.; Klemm, A.; Mao, H.; Pentzer, E.; Gurkan, B. Capsules of Reactive Ionic Liquids for Selective Capture of Carbon Dioxide at Low Concentrations. *ACS Appl. Mater. Interfaces* **2020**, *12* (16), 19184–19193. https://doi.org/10.1021/acsami.0c01622.
(11) Gaur, S. S.; Edgehouse, K. J.; Klemm, A.; Wei, P.; Gurkan, B.; Pentzer, E. B. Capsules with Polyurea Shells and Ionic Liquid Cores for CO_2 Capture. *Journal of Polymer Science* **2021**, *59* (23), 2980–2989. https://doi.org/10.1002/pol.20210342.
(12) Edgehouse, K. J.; Rosenfeld, N.; Bergbreiter, D. E.; Pentzer, E. B. Capsules of the Poly(α-Olefin) PAO_{432} for Removal of BTEX Contaminants from Water. *Ind. Eng. Chem. Res.* **2021**, *60* (40), 14455–14463. https://doi.org/10.1021/acs.iecr.1c02819.
(13) Ye, W.; Wang, N.; Hu, K.; Zhang, L.; Liu, A.; Pan, C.; Gong, T.; Liu, T.; Ding, H. Bio-Inspired Microcapsule for Targeted Antithrombotic Drug Delivery. *RSC Adv.* **2018**, *8* (48), 27253–27259. https://doi.org/10.1039/C8RA04273J.
(14) Lengyel, M.; Kállai-Szabó, N.; Antal, V.; Laki, A. J.; Antal, I. Microparticles, Microspheres, and Microcapsules for Advanced Drug Delivery. *Sci. Pharm.* **2019**, *87* (3), 20. https://doi.org/10.3390/scipharm87030020.
(15) Pentzer, E.; Cruz Barrios, E.; Starvaggi, N. Pickering Emulsions as Templates for Architecting Composite Structures. *Acc. Mater. Res.* **2023**, *4* (8), 641–647. https://doi.org/10.1021/accountsmr.3c00058.
(16) Capek, I. Degradation of Kinetically-Stable o/w Emulsions. *Advances in Colloid and Interface Science* **2004**, *107* (2–3), 125–155. https://doi.org/10.1016/S0001-8686(03)00115-5.

(17) Velikov, K. P.; Velev, O. D.; Marinova, K. G.; Constantinides, G. N. Effect of the Surfactant Concentration on the Kinetic Stability of Thin Foam and Emulsion Films. *Faraday Trans.* **1997**, *93* (11), 2069–2075. https://doi.org/10.1039/a608305f.
(18) Barnes, T. J.; Prestidge, C. A. PEO−PPO−PEO Block Copolymers at the Emulsion Droplet−Water Interface. *Langmuir* **2000**, *16* (9), 4116–4121. https://doi.org/10.1021/la991217d.
(19) Separation of Solids in the Surface-Layers of Solutions and 'Suspensions' (Observations on Surface-Membranes, Bubbles, Emulsions, and Mechanical Coagulation).—Preliminary Account. *Proc. R. Soc. Lond.* **1904**, *72* (477–486), 156–164. https://doi.org/10.1098/rspl.1903.0034.
(20) Pickering, S. U. CXCVI.—Emulsions. *J. Chem. Soc., Trans.* **1907**, *91* (0), 2001–2021. https://doi.org/10.1039/CT9079102001.
(21) Yang, Y.; Fang, Z.; Chen, X.; Zhang, W.; Xie, Y.; Chen, Y.; Liu, Z.; Yuan, W. An Overview of Pickering Emulsions: Solid-Particle Materials, Classification, Morphology, and Applications. *Front. Pharmacol.* **2017**, *8*, 287. https://doi.org/10.3389/fphar.2017.00287.
(22) Wei, P.; Luo, Q.; Edgehouse, K. J.; Hemmingsen, C. M.; Rodier, B. J.; Pentzer, E. B. 2D Particles at Fluid–Fluid Interfaces: Assembly and Templating of Hybrid Structures for Advanced Applications. *ACS Appl. Mater. Interfaces* **2018**, *10* (26), 21765–21781. https://doi.org/10.1021/acsami.8b07178.
(23) Kim, J.; Cote, L. J.; Kim, F.; Yuan, W.; Shull, K. R.; Huang, J. Graphene Oxide Sheets at Interfaces. *J. Am. Chem. Soc.* **2010**, *132* (23), 8180–8186. https://doi.org/10.1021/ja102777p.
(24) Che Man, S. H.; Mohd Yusof, N. Y.; Whittaker, M. R.; Thickett, S. C.; Zetterlund, P. B. Influence of Monomer Type on Miniemulsion Polymerization Systems Stabilized by Graphene Oxide as Sole Surfactant. *J. Polym. Sci. Part A: Polym. Chem.* **2013**, *51* (23), 5153–5162. https://doi.org/10.1002/pola.26947.
(25) Dong, J.; Worthen, A. J.; Foster, L. M.; Chen, Y.; Cornell, K. A.; Bryant, S. L.; Truskett, T. M.; Bielawski, C. W.; Johnston, K. P. Modified Montmorillonite Clay Microparticles for Stable Oil-in-Seawater Emulsions. *ACS Appl. Mater. Interfaces* **2014**, *6* (14), 11502–11513. https://doi.org/10.1021/am502187t.
(26) Dai, H.; Wu, J.; Zhang, H.; Chen, Y.; Ma, L.; Huang, H.; Huang, Y.; Zhang, Y. Recent Advances on Cellulose Nanocrystals for Pickering Emulsions: Development and Challenge. *Trends in Food Science & Technology* **2020**, *102*, 16–29. https://doi.org/10.1016/j.tifs.2020.05.016.
(27) Alison, L.; Demirörs, A. F.; Tervoort, E.; Teleki, A.; Vermant, J.; Studart, A. R. Emulsions Stabilized by Chitosan-Modified Silica Nanoparticles: PH Control of Structure–Property Relations. *Langmuir* **2018**, *34* (21), 6147–6160. https://doi.org/10.1021/acs.langmuir.8b00622.
(28) Ruckenstein, E. Microemulsions, Macroemulsions, and the Bancroft Rule. *Langmuir* **1996**, *12* (26), 6351–6353. https://doi.org/10.1021/la960849m.
(29) Wu, J.; Ma, G.-H. Recent Studies of Pickering Emulsions: Particles Make the Difference. *Small* **2016**, *12* (34), 4633–4648. https://doi.org/10.1002/smll.201600877.
(30) Binks, B. P.; Lumsdon, S. O. Stability of Oil-in-Water Emulsions Stabilised by Silica Particles. *Phys. Chem. Chem. Phys.* **1999**, *1* (12), 3007–3016. https://doi.org/10.1039/a902209k.

(31) Sadeghpour, A.; Pirolt, F.; Glatter, O. Submicrometer-Sized Pickering Emulsions Stabilized by Silica Nanoparticles with Adsorbed Oleic Acid. *Langmuir* **2013**, *29* (20), 6004–6012. https://doi.org/10.1021/la4008685.
(32) Saigal, T.; Dong, H.; Matyjaszewski, K.; Tilton, R. D. Pickering Emulsions Stabilized by Nanoparticles with Thermally Responsive Grafted Polymer Brushes. *Langmuir* **2010**, *26* (19), 15200–15209. https://doi.org/10.1021/la1027898.
(33) Schoth, A.; Landfester, K.; Muñoz-Espí, R. Surfactant-Free Polyurethane Nanocapsules via Inverse Pickering Miniemulsion. *Langmuir* **2015**, *31* (13), 3784–3788. https://doi.org/10.1021/acs.langmuir.5b00442.
(34) Graham, M.; Shchukin, D. Formation Mechanism of Multipurpose Silica Nanocapsules. *Langmuir* **2021**, *37* (2), 918–927. https://doi.org/10.1021/acs.langmuir.0c03286.
(35) Issa, A.; Luyt, A. Kinetics of Alkoxysilanes and Organoalkoxysilanes Polymerization: A Review. *Polymers* **2019**, *11* (3), 537. https://doi.org/10.3390/polym11030537.
(36) McElwee, J.; Helmy, R.; Fadeev, A. Y. Thermal Stability of Organic Monolayers Chemically Grafted to Minerals. *Journal of Colloid and Interface Science* **2005**, *285* (2), 551–556. https://doi.org/10.1016/j.jcis.2004.12.006.
(37) Walstra, P., in Encyclopedia of Emulsion Technology, Vol. 1, P. Becher (Ed.), Pp.57-128, Marcel Dekker, New York, 1983.
(38) Wang, B.; Zhang, Z.; Feng, W.; Luo, J.; Shi, S. Stabilizing and Structuring Oil–Oil Interfaces by Molecular Brush Surfactants: Special Issue: Emerging Investigators. *Aggregate* **2022**, *3* (6). https://doi.org/10.1002/agt2.292.
(39) Binks, B. P.; Lumsdon, S. O. Catastrophic Phase Inversion of Water-in-Oil Emulsions Stabilized by Hydrophobic Silica. *Langmuir* **2000**, *16* (6), 2539–2547. https://doi.org/10.1021/la991081j.
(40) Yi-Wei, F.; Shao-Jun, R.; Jun, M.; Feng, G. Study on Thermal Oxidation and Viscosity Degradation for Synthetic Aviation Lubricant Fluids. *IOP Conf. Ser.: Mater. Sci. Eng.* **2020**, *729* (1), 012072. https://doi.org/10.1088/1757-899X/729/1/012072.
(41) Talaty, E. R.; Raja, S.; Storhaug, V. J.; Dölle, A.; Carper, W. R. Raman and Infrared Spectra and Ab Initio Calculations of C_{2-4} MIM Imidazolium Hexafluorophosphate Ionic Liquids. *J. Phys. Chem. B* **2004**, *108* (35), 13177–13184. https://doi.org/10.1021/jp040199s.